Biochemistry

 Volume 40, Number 6 February 13, 2001

Accelerated Publications

Flash-Induced Fourier Transform Infrared Detection of the Structural Changes during the S-State Cycle of the Oxygen-Evolving Complex in Photosystem II

Takumi Noguchi*,‡ and Miwa Sugiura§

Biophysical Chemistry Laboratory, RIKEN, Wako, Saitama 351-0198, Japan, and Department of Applied Biological Chemistry, Faculty of Agriculture, Osaka Prefecture University, 1-1 Gakuen-cho, Sakai, Osaka 599-8531, Japan

Received October 13, 2000; Revised Manuscript Received November 27, 2000

ABSTRACT: Fourier transform infrared (FTIR) difference spectra of all flash-induced S-state transitions of the oxygen-evolving complex were measured using photosystem II (PSII) core complexes of *Synechococcus elongatus*. The PSII core sample was given eight successive flashes with 1 s intervals at 10 °C, and FTIR difference spectra upon individual flashes were measured. The obtained difference spectra upon the first to fourth flashes showed considerably different spectral features from each other, whereas the fifth, sixth, seventh, and eighth flash spectra were similar to the first, second, third, and fourth flash spectra, respectively. The intensities at the wavenumbers of prominent peaks of the first and second flash spectra showed clear period four oscillation patterns. These oscillation patterns were well fitted with the Kok model with 13% misses. These results indicate that the first, second, third, and fourth flash spectra represent the difference spectra upon the $S_1 \rightarrow S_2$, $S_2 \rightarrow S_3$, $S_3 \rightarrow S_0$, and $S_0 \rightarrow S_1$ transitions, respectively. In these spectra, prominent bands were observed in the symmetric (1300−1450 cm^{-1}) and asymmetric (1500−1600 cm^{-1}) stretching regions of carboxylate groups and in the amide I region (1600−1700 cm^{-1}). Comparison of the band features suggests that the drastic coordination changes of carboxylate groups and the protein conformational changes in the $S_1 \rightarrow S_2$ and $S_2 \rightarrow S_3$ transitions are reversed in the $S_3 \rightarrow S_0$ and $S_0 \rightarrow S_1$ transitions. The flash-induced FTIR measurements during the S-state cycle will be a promising method to investigate the detailed molecular mechanism of photosynthetic oxygen evolution.

Photosynthetic oxygen evolution is performed in photosystem II (PSII)[1] of plants and cyanobacteria. The catalytic center of this reaction is the oxygen-evolving complex (OEC), which resides on the electron donor side of PSII (reviewed in refs *1*−*7*). The OEC has a core structure of the tetranuclear Mn cluster, which consists of four Mn ions and one Ca ion connected by μ-oxo and amino acid ligands. In OEC, two water molecules are oxidized to cleave into one oxygen molecule and four protons. This reaction proceeds through a light-driven cycle called the S-state cycle (*8*, *9*), which consists of five intermediates, S_0−S_4. Upon excitation of PSII by a single-turnover flash, the primary donor P_{680} abstracts an electron from OEC through Y_Z, and the dark stable S_1 state is advanced to the S_2 state. Likewise, by subsequent flashes, the S_2 state is advanced to the S_3 and to the S_0 state and returns to the S_1 state. Molecular oxygen is

* To whom correspondence should be addressed. Phone: +81-48-462-1111 ext 5461. Fax: +81-48-462-4660. E-mail: tnoguchi@postman.riken.go.jp.

‡ RIKEN.

§ Osaka Prefecture University.

[1] Abbreviations: DM, *n*-dodecyl β-D-maltoside; FTIR, Fourier transform infrared; fwhm, full width at half-maximum; IR, infrared; Mes, 2-(*N*-morpholino)ethanesulfonic acid; OEC, oxygen-evolving complex; PSII, photosystem II.

10.1021/bi0023807 CCC: $20.00
Published on Web 01/04/2001

evolved in the $S_3 \rightarrow S_0$ transition though the unstable S_4 state. Thus, in dark-adapted PSII, oxygen is released after the first three flashes, and afterward, the period four oscillation of oxygen evolution is observed. Although this concept of the S-state cycle has been well established, the detailed structure of OEC in the individual S-state intermediates, the molecular mechanism of oxygen evolution, and the involvement of proteins in the reactions mostly remain to be clarified.

FTIR difference spectroscopy is a powerful method to study the molecular structures of the active sites of proteins and their enzymatic reactions. This method is especially useful to photosensitive proteins such as photosynthetic reaction centers (*10*, *11*) and rhodopsins (*12*, *13*), because light illumination can be used as a trigger to start reactions. For these proteins, the structures of cofactors, active amino acid residues, and protein conformations as well as hydrogen-bonding interactions and proton-transfer reactions have been studied. One of the merits of FTIR difference spectroscopy is that basically all of the structural changes upon the reaction are detected in spectra. This is in contrast to EXAFS, EPR, and resonance Raman spectroscopies, which specifically detect the metal centers, paramagnetic species, or pigments.

FTIR difference spectroscopy has been applied to the research of photosynthetic oxygen evolution these several years (*14*−*27*). So far, almost all of the difference spectra have been measured upon the first $S_1 \rightarrow S_2$ transition (*14*−*26*), because the S_2 state can be produced with a high yield and stabilized at cryogenic temperatures (typically at 250 K). Analyses of the S_2/S_1 difference spectra in the mid-IR region of 1800−1000 cm^{-1} have revealed the presence of carboxylate ligands (*14*−*17*, *19*), the protonation and hydrogen-bonding structure of a histidine ligand (*19*), changes in conformations of the polypeptide chains (*14*, *16*, *17*), and the structural coupling of a tyrosine residue with the Mn cluster (*18*). Recently, we have detected the O−H stretching bands of an active water in OEC at 3618/3585 cm^{-1} and discussed its hydrogen-bonding structure (*22*). Chu et al. (*24*−*26*) reported the S_2/S_1 spectrum in the lower frequency region of 1000−350 cm^{-1}, where the Mn−ligand and Mn−substrate vibrations are expected to be present. Very recently, Chu et al. (*27*) reported the S_3/S_2 spectrum in the mid-IR region.

To investigate the molecular mechanism of oxygen evolution, it is essential to detect the structural changes and reactions in all of the S-state transitions. The $S_3 \rightarrow S_0$ transition is of particular interest because in this transition an O−O bond is created and molecular oxygen is released. FTIR measurements of the S-state transitions other than $S_1 \rightarrow S_2$ have been hampered by (i) their high inhibition temperatures [the $S_2 \rightarrow S_3$, $S_3 \rightarrow S_0$, and $S_0 \rightarrow S_1$ transitions fully proceed above 265, 270, and 250 K, respectively, in contrast to above 200 K in the $S_1 \rightarrow S_2$ transition (*28*)], (ii) the shorter lifetimes of the S_2 and S_3 states at higher temperature, (iii) unstable baselines of FTIR difference spectra for liquid samples, preventing long data accumulation, and (iv) the mixture of more than one S-state transition due to misses. In this study, we have measured flash-induced FTIR difference spectra during the S-state cycle by overcoming the above difficulties by adopting a sample temperature of 10 °C and a short scan time of 1 s between flashes. To improve the S/N ratio, the cycle of a flash train and subsequent dark adaptation was repeated and the spectra were averaged. To avoid sample damage by long measurement at the relatively high temperature, we used the highly stable PSII core complexes prepared from the thermophilic cyanobacterium *Synechococcus elongatus*. The observed FTIR signals showed clear period four oscillation patterns, and thus the obtained flash-induced spectra reveal the differences upon the individual S-state transitions ($S_1 \rightarrow S_2$, $S_2 \rightarrow S_3$, $S_3 \rightarrow S_0$, and $S_0 \rightarrow S_1$). The results in this study will open the way to the investigation of the molecular mechanism of photosynthetic oxygen evolution.

MATERIALS AND METHODS

Oxygen-evolving PSII core complexes from *S. elongatus*, in which the carboxyl terminus of the CP43 subunit was genetically histidine-tagged, were purified using Ni^{2+}-affinity column chromatography as described by Sugiura and Inoue (*29*). The typical value of oxygen-evolving activity of this PSII core was 2200 μmol (mg of Chl)$^{-1}$ h^{-1} at 25 °C with ferricyanide as an exogenous electron acceptor (*29*). This core complex is also highly stable and retains more than 90% of the original oxygen-evolving activity even after 8 day incubation at 20 °C (*29*). The PSII core complexes were suspended in 40 mM Mes−NaOH buffer (pH. 6.5) containing 20 mM NaCl, 15 mM $CaCl_2$, 15 mM $MgCl_2$, 0.03% DM, and 25% glycerol and stored in liquid N_2 until use. For FTIR measurements, the buffer was exchanged for 10 mM Mes−NaOH (pH 6.0) containing 50 mM sucrose, 5 mM NaCl, 5 mM $CaCl_2$, and 0.06% DM by repeating concentration and resuspension using Microcon-100 (Amicon).

FTIR spectra were measured on a Bruker IFS-66/S spectrophotometer equipped with an MCT detector (EG&G JUDSON, J15D16-M200B-S01M-60). An aliquot of the core suspension (4.5 mg of Chl/mL; 10 μL) was mixed with 2.4 μL of 100 mM potassium ferricyanide solution and placed on a CaF_2 plate. The sample was then lightly dried under N_2 gas flow, hydrated with 0.6 μL of water, and covered with another CaF_2 plate. These CaF_2 plates (25 mm $\phi \times 3$ mm) have a circular groove (14 mm inner diameter; 1 mm width; 0.5 mm depth), and the sample was placed in the inner area of the groove. In the outer part of the groove, silicone grease was placed between the two plates to seal the sample (*30*). Absorbance of the peak around 1650 cm^{-1} due to the amide I and water bands was adjusted to about 1.0. The sample temperature was kept at 10 °C by circulating cool water through a copper sample holder. A Ge filter (OCLI, LO2584-9) was placed in front of the sample in the IR-beam path to block the red light of the He−Ne laser leaking from the interferometer. Flash illumination was performed by nanosecond pulses from a frequency-doubled Q-switched Nd:YAG laser (Quanta-Ray GCR-130; 532 nm; ∼7 ns fwhm). The pulse energy was ∼10 mJ/(pulse cm^2) at the sample point, which was ensured to saturate the PSII turnover by examining the amplitude of a single-flash-induced FTIR spectrum as a function of the pulse energy. Flash-induced FTIR measurement during the S-state cycle of OEC was performed by repeating the cycle of flash illumination and dark adaptation as in the scheme presented in Figure 1. The dark-adapted sample was given eight successive flashes with 1 s intervals, and nine single-beam spectra [single-sided forward/backward; two scans (1 s accumulation) for each] were measured before the first flash, between the flashes, and after the eighth flash using the rapid scan mode. The

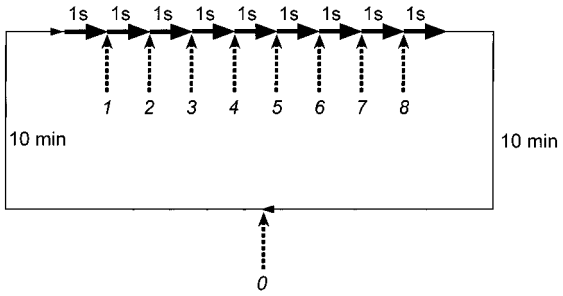

FIGURE 1: Scheme of flash-induced FTIR measurement during the S-state cycle of OEC. Thick arrows indicate FTIR scans, and dotted arrows indicate the flash illumination by laser pulses (532 nm; ~7 ns fwhm). The PSII sample was given eight successive flashes with 1 s intervals. FTIR spectra were measured for 1 s before the first flash, between the flashes, and after the eighth flash. After dark adaptation for 10 min, another flash was applied followed by further dark adaptation for 10 min to synchronize all the oxygen-evolving centers to the S_1 state. This measurement cycle was repeated, and spectra were averaged.

sample was then dark adapted for 10 min to relax the S_2 and S_3 states to the S_1 state, followed by application of another flash to advance the partially populated S_0 state to the S_1 state. The sample was further dark adapted for 10 min to synchronize all the OEC into the S_1 state. This 10 min dark time was determined from the lifetimes ($\tau_{1/2}$) of the S_2 and S_3 states, which were roughly estimated to be shorter than 3 min under the sample condition used by detecting the decay of the FTIR signals induced upon one or two flashes. This measurement cycle was repeated less than 30 times for each sample. Eight independent samples were measured, and the spectra by 232 cycles were averaged. Difference spectra upon the first to eighth flashes were calculated as a difference between the single-beam spectra measured before and after each flash. The spectral resolution was 4 cm^{-1}. Least-squares fitting of the oscillation patterns was performed utilizing the built-in fitting operation of the IGOR Pro program (Wavemetrics Inc.).

RESULTS AND DISCUSSION

Figure 2 shows FTIR difference spectra of the PSII core complexes from *S. elongatus* upon illumination of the first to eighth flashes measured at 10 °C. Because the sample solution includes ferricyanide as an exogenous electron acceptor, only the structural changes by the S-state advancement in OEC are revealed in the spectra. In fact, negative and positive peaks at 2115 and 2038 cm^{-1} due to ferricyanide and ferrocyanide, respectively, are observed in all of the spectra (not shown), indicating abstraction of an electron by ferricyanide upon each flash. The spectra upon the first to fourth flashes (Figure 2a−c, thick lines) showed significantly different features from each other. By contrast, the fifth, sixth, seventh, and eighth flash spectra (Figure 2a−d, thin lines) have basically the same features as the first, second, third, and fourth flash spectra (Figure 2a−d, thick lines), respectively, although the overall spectral intensities of the fifth to eighth flash spectra are smaller than those of the corresponding first to fourth flash spectra. This observation indicates that the individual S states are advanced properly to the next S states by saturating flashes, and the period four cycle of the S states works well under the present measuring condition (Figure 1).

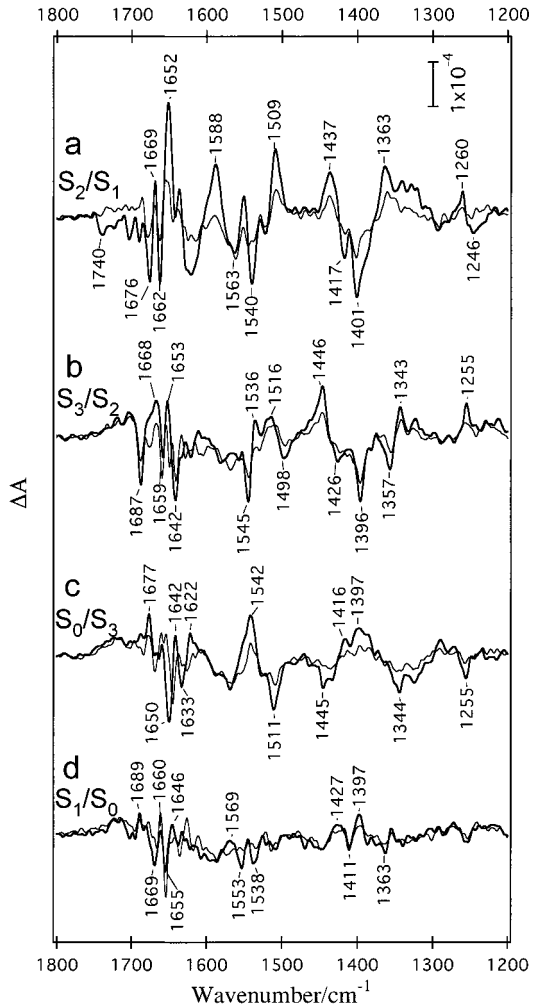

FIGURE 2: Flash-induced FTIR difference spectra (after-minus-before each flash) of OEC in the PSII core complexes from *S. elongatus*. Difference spectra upon the first and fifth (a), second and sixth (b), third and seventh (c), and fourth and eighth (d) flashes are presented in thick (first−fourth flash) and thin (fifth−eighth flash) lines. The spectra in (a), (b), (c), and (d) virtually represent the S_2/S_1, S_3/S_2, S_0/S_3, and S_1/S_0 difference, respectively. The sample included ferricyanide as an exogenous electron acceptor. The measurement was performed following the scheme in Figure 1. The sample temperature was 10 °C. Flash illumination was given by a pulse (532 nm; ~7 ns fwhm) from a Nd:YAG laser with an energy of ~10 mJ/(pulse cm^2). The spectral resolution was 4 cm^{-1}.

The difference spectrum upon the first flash (Figure 2a, thick line) should exhibit only the S_2/S_1 difference, and indeed it is virtually identical to the S_2/S_1 difference spectrum measured at 250 K using the same PSII core complex of *S. elongatus* (*22*) and is very similar to the spectra using the PSII membranes or core preparations from spinach (*14*−*17*, *21*, *24*) and *Synechocystis* 6803 (*18*, *19*). The second and sixth flash spectra (Figure 2b) are similar to the S_3/S_2 spectrum at 250 K, which was very recently reported by Chu et al. (*27*). The bands at 1545, 1446, 1396, and 1357 cm^{-1} in the spectra of Figure 2b correspond to the bands at 1545, 1445, 1399, and 1355 cm^{-1}, respectively, in their spectra. This observation is consistent with the expectation that the $S_2 \rightarrow S_3$ transition largely takes place by the second and sixth flashes. The third and seventh flash spectra (Figure 2c) and the fourth and eighth flash spectra (Figure 2d) are expected to include the largest contributions of the S_0/S_3 and S_1/S_0 differences, respectively.

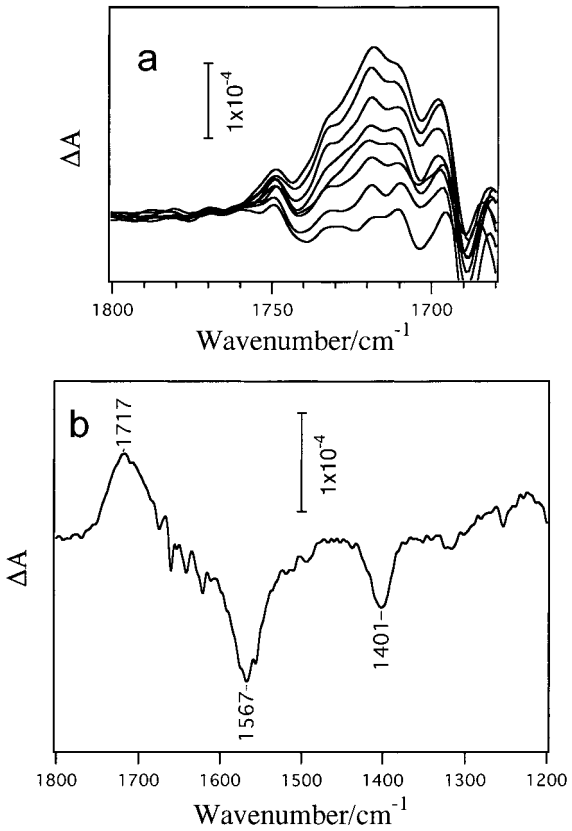

FIGURE 3: (a) Flash-induced FTIR difference spectra of OEC in the COOH region obtained by subtraction of the spectrum before the first flash from those after the first to eighth flashes (from lower to higher spectra). The raw spectra used for calculation of the difference spectra were the same as those for Figure 2. (b) Flash-induced FTIR difference spectrum of OEC with randomized S states. The measurement was performed by the cycle of four successive flashes (1 Hz), the first 10 s scans, another four flashes (1 Hz), and the second 10 s scans. The flash was given by a laser pulse with an energy of ~2.0 mJ/(pulse cm^2), which induces about half of the PSII turnover. The difference spectrum was calculated between the first and the second 10 s spectra. The cycle was repeated 50 times, and the spectra were averaged. The sample temperature was 10 °C.

On closer inspection, it is found that all of the spectra in Figure 2 except for the first flash spectrum show a broad positive feature around 1720 cm^{-1}. This positive feature is more clearly seen in the difference spectra between before the first flash and after the *n*th flash ($n = 1-8$) (Figure 3a). The broad band around 1720 cm^{-1} increases stepwise as the flash number increases. To examine whether this feature is related to the particular S-state transitions, a flash-induced difference spectrum was measured for OEC in randomized S states. The measurement was performed by the cycle of four successive flashes (1 Hz), the first FTIR scans for 10 s, another four flashes (1 Hz), and the second FTIR scans for 10 s. The flash was given by a laser pulse with an energy of ~2.0 mJ/(pulse cm^2), which induces about half of the PSII turnover. Repeating this cycle of a series of nonsaturating flashes makes the S states in OEC always randomized. The difference spectrum was calculated between the first and the second 10 s spectra. The cycle was repeated 50 times, and the difference spectra were averaged. The resultant FTIR difference spectrum should exhibit flash-induced changes in the sample but not specific to individual S-state transitions.

Figure 3b shows the obtained FTIR difference spectrum. The prominent negative bands at 1567 and 1401 cm^{-1} and a positive band at 1717 cm^{-1} were observed. These spectral changes are typical of the protonation reaction of caboxylate groups; the bands at 1567 and 1401 cm^{-1} are ascribed to the asymmetric and symmetric COO^- stretching vibrations, respectively, and the 1717 cm^{-1} band is due to the C=O stretching vibration of a COOH group. Because no components of the medium (Mes, sucrose, DM, NaCl, and $CaCl_2$) include a carboxylate group, these bands are considered to arise from the PSII protein itself. From the observation that the bands are relatively broad and no specific structures are found, it is assumed that these bands come from nonspecific carboxylate groups of amino acid residues in the proteins. Probably, a slight pH decrease of the medium by proton release from OEC during the S-state turnover causes the protonation of carboxylate groups in the hydrophilic region of the PSII proteins. It has been shown that the proton release pattern for the S-state transitions varies by materials and pH (*31*), and in the case of the core complexes of *S. elongatus*, the proton release stoichiometry was reported to be 1.0:0.2:1.0:1.8 for the $S_0 \rightarrow S_1 \rightarrow S_2 \rightarrow S_3 \rightarrow S_0$ transitions at pH 6 (*32*). The observation that the positive feature around 1720 cm^{-1} has little intensity in the first flash spectrum and afterward the intensity increases by a similar amount upon accumulation of flashes (Figure 3a) is basically consistent with this proton release stoichiometry. The absence of a clear oscillation pattern in the intensity around 1720 cm^{-1} is probably due to the buffering effect of the medium used.

Figure 4 shows the flash-induced oscillation patterns of the intensities at 1363 (a), 1401 (b), 1509 (c), 1396 (d), 1446 (e), and 1545 (f) cm^{-1} in the FTIR difference spectra upon the first to eighth flashes (Figure 2). The former three (a−c) and the latter three (d−f) wavenumbers are the positions of the selected prominent peaks of the first flash (S_2/S_1; Figure 2a, thick line) and the second flash (largely S_3/S_2; Figure 2b, thick line) spectra, respectively. Before the data were plotted, the spectra in Figure 2 except for the first flash spectrum were corrected for the COOH/COO^- bands; the spectrum of Figure 3b was subtracted from each spectrum of Figure 2. In this subtraction, the amplitude of the COOH/COO^- spectrum (Figure 3b) was scaled for each flash-induced spectrum (Figure 2) so that the resultant spectrum has a flat baseline above 1700 cm^{-1}.

The plots of the experimental data (filled circles with solid lines) show clear period four oscillations. In the flash-induced patterns of 1363, 1401, and 1509 cm^{-1} (Figure 4a−c), strong positive or negative intensities are observed at the first and the fifth flash, while in the patterns of 1396, 1446, and 1545 cm^{-1} (Figure 4d−f), strong intensities are observed at the second and the sixth flash. Also, the prominent positive peaks at 1397 and 1542 cm^{-1} and negative peaks at 1445 and 1511 cm^{-1} observed in the third flash spectrum (Figure 2c, thick line) are expressed as strong intensities at the third and the seventh flash in the oscillation patterns of 1396, 1545, 1446, and 1509 cm^{-1} (panels d, f, e, and c of Figure 4), respectively.

The above oscillation patterns were analyzed by fitting with the Kok model (*8*, *9*) assuming a miss parameter (*m*). The double hits are considered to be zero, because the laser pulse with an about 7 ns width (fwhm) was used for excitation and there is no possibility that two turnover

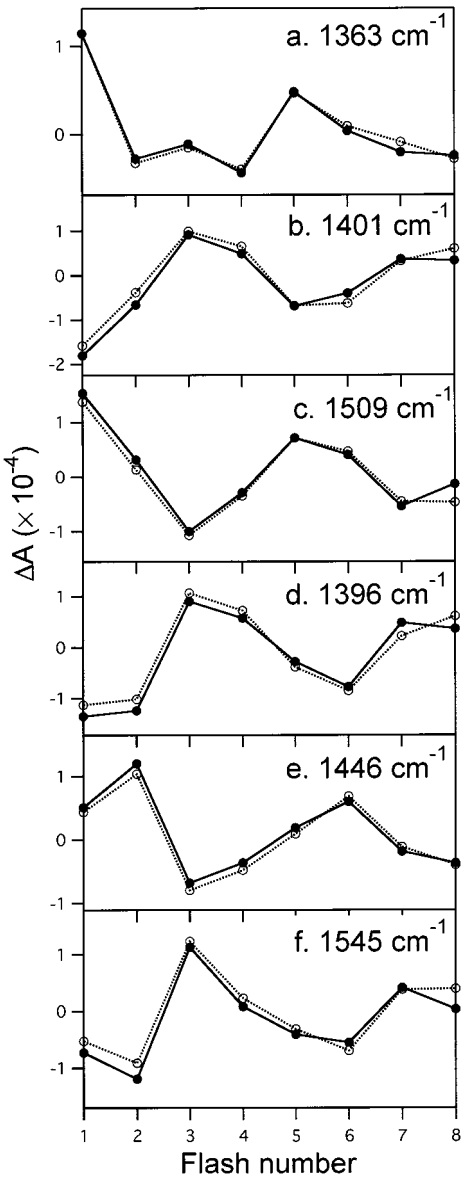

FIGURE 4: Flash-induced oscillation patterns of the FTIR intensities (ΔA) at 1363 (a), 1401 (b), 1509 (c), 1396 (d), 1446 (e), and 1545 (f) cm^{-1}. The ΔA values at each wavenumber were taken from the FTIR difference spectra upon the first−eighth flashes (Figure 2) after correction for the unspecific $COOH/COO^-$ contribution (Figure 3) (see text). The wavenumers of (a)−(c) and (d)−(f) are the positions of the selected prominent peaks in the difference spectra upon the first and the second flashes, respectively. Filled circles with solid lines indicate the experimental data, and open circles with dotted lines are the best fit of the oscillation patterns with 13% misses.

reactions take place in OEC in the early nanosecond time scale. An absorbance change at a certain wavenumber (ν) upon the nth flash is expressed as

$$\Delta A_n(\nu) = \Delta p_{0n} A_0(\nu) + \Delta p_{1n} A_1(\nu) + \Delta p_{2n} A_2(\nu) + \Delta p_{3n} A_3(\nu)$$

where $A_0(\nu)$, $A_1(\nu)$, $A_2(\nu)$, and $A_3(\nu)$ are the absolute absorbances at ν in the S_0, S_1, S_2, and S_3 states, respectively, and Δp_{0n}, Δp_{1n}, Δp_{2n}, and Δp_{3n} represent the nth-flash-induced changes in relative population of the S_0, S_1, S_2, and S_3 states, respectively. The values of Δp_{0n}, Δp_{1n}, Δp_{2n}, and Δp_{3n} are determined by the miss factor m. Using the relationship, $\Delta p_{0n} + \Delta p_{1n} + \Delta p_{2n} + \Delta p_{3n} = 0$, $\Delta A_n(\nu)$ is changed to

$$\Delta A_n(\nu) = \Delta p_{0n} \Delta A_{0-1}(\nu) + \Delta p_{2n} \Delta A_{2-1}(\nu) + \Delta p_{3n} \Delta A_{3-1}(\nu)$$

where $\Delta A_{0-1}(\nu)$, $\Delta A_{2-1}(\nu)$, and $\Delta A_{3-1}(\nu)$ are the absorbance differences at ν in the S_0, S_2, and S_3 states with respect to the absorbance in the S_1 state. Thus, the oscillation pattern of $\Delta A_n(\nu)$ can be fitted using the four parameters, m, $\Delta A_{0-1}(\nu)$, $\Delta A_{2-1}(\nu)$, and $\Delta A_{3-1}(\nu)$.

The data at all of the wavenumbers in Figure 4 were fitted simultaneously, and the best fit was obtained by $m = 13\%$. The resultant oscillation patterns of the best fit are shown as open circles with dotted lines in Figure 4. It is seen that the experimental oscillation patterns are well reproduced by the fitting. It is noted that, without correction for the $COOH/COO^-$ bands (Figure 3b), the oscillation patterns at 1401, 1396, and 1545 cm^{-1} could not be fitted satisfactorily.

The 13% misses explain the decrease in the overall intensities of the flash-induced spectra (Figure 2) as the flash number advances; the partial centers in which the S states are randomized mostly cancel out the intensities, and the major S-state transition by each flash is left in the spectrum. From the clear period four oscillation patterns together with the observation that the spectral features are considerably different among the first to fourth flash spectra (Figure 2a−d, thick lines), and each difference spectrum in the second cycle (Figure 2a−c, thin lines) has basically the same band features as the corresponding spectrum in the first cycle (Figure 2a−d, thick lines), it is considered that the first, second, third, and fourth flash spectra virtually express the S_2/S_1, S_3/S_2, S_0/S_3, and S_1/S_0 spectra, respectively.

In all of the first to fourth flash spectra (Figure 2), prominent bands are observed in the symmetric (1300−1450 cm^{-1}) and asymmetric (1500−1600 cm^{-1}) stretching regions of carboxylate groups, suggesting that drastic structural changes of the carboxylate ligands occur in all of the S-state transitions. The band frequencies in the carboxylate regions are rather different between the S_2/S_1 and S_3/S_2 spectra (Figure 2a,b), indicating that different carboxylate groups react in the $S_1 \rightarrow S_2$ and $S_2 \rightarrow S_3$ transitions. It seems that these carboxylate changes in $S_1 \rightarrow S_2$ and $S_2 \rightarrow S_3$ are reversed in the $S_3 \rightarrow S_0$ and $S_0 \rightarrow S_1$ transitions, because in the S_0/S_3 and S_1/S_0 spectra (spectra c and d of Figure 2, respectively), bands are observed at the similar frequencies to the bands in the S_2/S_1 and S_3/S_2 spectra (spectra a and b of Figure 2, respectively) with opposite signs. The negative peaks at 1401 and 1396 cm^{-1} in the S_2/S_1 and S_3/S_2 spectra, respectively, may correspond to the positive bands at 1397 cm^{-1} in the S_0/S_3 and S_1/S_0 spectra. Also, the negative peaks at 1417 (S_2/S_1), 1426 (S_3/S_2), and 1545 (S_3/S_2) cm^{-1} correspond to the positive peaks at 1416 (S_0/S_3), 1427 (S_1/S_0), and 1542 (S_0/S_3) cm^{-1}, respectively. In addition, the positive peaks at 1343 (S_3/S_2), 1363 (S_2/S_1), 1446 (S_3/S_2), and 1509 (S_2/S_1) cm^{-1} seem to be the counterparts of the negative peaks at 1344 (S_0/S_3), 1363 (S_1/S_0), 1445 (S_0/S_3), and 1511 (S_0/S_3) cm^{-1}, respectively. The straightforward interpretation of these drastic changes in the carboxylate groups upon the S-state transitions is that the coordination structures of the carboxylate ligands of the Mn and/or Ca ions significantly change during the S-state cycle. It is also

possible that some carboxylate groups that are not the ligands of the metal ions undergo significant changes in their hydrogen-bonding interactions. In either case, the observed drastic structural changes may indicate the possibility that some carboxylate groups of the proteins are directly involved in the reaction mechanism of oxygen evolution (e.g., as proton abstractors or proton-transfer mediators) rather than simply work as structural constituents of OEC.

In the amide I region (1600−1700 cm^{-1}), where protein conformational changes are revealed, the band intensities are more or less similar in all of the spectra of individual S-state transitions (Figure 2). This means that there is no specific S-state transition that brings about especially large conformational changes of proteins. Similarly to the bands in the carboxylate region, the band pattern in the amide I region is significantly different between the S_2/S_1 and S_3/S_2 spectra (spectra a and b of Figure 2, respectively) and the band changes seem to be reversed in the S_0/S_3 and S_1/S_0 spectra (spectra c and d of Figure 2, respectively). The positive bands at 1652 and 1669 cm^{-1} (S_2/S_1) and the negative bands at 1642 (S_3/S_2), 1662 (S_2/S_1), 1676 (S_2/S_1), and 1687 (S_3/S_2) cm^{-1} correspond to the negative bands at 1650 (S_0/S_3) and 1669 (S_1/S_0) cm^{-1} and the positive bands at 1642 (S_0/S_3), 1660 (S_1/S_0), 1677 (S_0/S_3), and 1689 (S_1/S_0) cm^{-1}, respectively.

Relatively strong peaks are observed at 1255 cm^{-1} in the S_3/S_2 and S_0/S_3 spectra with opposite signs (Figure 2b,c). Previously, it was shown that the S_2/S_1 spectrum has a negative peak at 1255 cm^{-1} (hidden in the band feature at 1260/1246 cm^{-1} in Figure 2a) arising from a tyrosine side chain, most likely Y_Z, coupled to the Mn cluster through a hydrogen bond network (*18*). It is possible that the peaks at 1255 cm^{-1} in the S_3/S_2 and S_0/S_3 spectra also come from Y_Z, suggesting that the interaction between the Mn cluster and Y_Z changes during these transitions.

CONCLUDING REMARKS

We have measured FTIR difference spectra during the flash-induced S-state cycle of OEC. The FTIR signals showed clear period four oscillation patterns, and the obtained first, second, third, and fourth flash spectra reveal the differences upon the $S_1 \rightarrow S_2$, $S_2 \rightarrow S_3$, $S_3 \rightarrow S_0$, and $S_0 \rightarrow S_1$ transitions, respectively. These difference spectra include the information of structural changes and chemical reactions of the proteins and substrate during the S-state cycle. Because the measurements are performed at 10 °C, the reactions in OEC can be followed under physiological conditions. Careful analysis of the spectra using isotopic labeling and site-directed mutants is expected to provide the details of the reactions of substrate water and individual amino acid residues. Thus, flash-induced FTIR difference measurements in the S-state cycle of OEC will be a promising method to investigate the molecular mechanism of the photosynthetic oxygen evolution.

REFERENCES

1. Debus, R. J. (1992) *Biochim. Biophys. Acta 1102*, 269−352.
2. Britt, R. D. (1996) in *Oxygenic Photosynthesis: The Light Reactions* (Ort, D. R., and Yocum, C. F., Eds.) pp 137−164, Kluwer, Dordrecht, The Netherlands.
3. Yachandra, V. K., Sauer, K., and Klein, M. P. (1996) *Chem. Rev. 96*, 2927−2950.
4. Renger, G. (1997) *Physiol. Plant. 100*, 824−841.
5. Rüttinger, W., and Dismukes, G. C. (1997) *Chem. Rev. 97*, 1−24.
6. Tommos, C., and Babcock, G. T. (1998) *Acc. Chem. Res. 31*, 18−25.
7. Renger, G. (2000) *Biochim. Biophys. Acta* (in press).
8. Joliot, P., Barbieri, G., and Chabaud, R. (1969) *Photochem. Photobiol. 10*, 309−329.
9. Kok, B., Forbush, B., and McGloin, M. (1970) *Photochem. Photobiol. 11*, 457−475.
10. Mäntele, W. G. (1995) in *Anoxygenic Photosynthetic Bacteria* (Blankenship, R. E., Madigan, M. T., and Bauer, C. E., Eds.) pp 627−647, Kluwer, Dordrecht, The Netherlands.
11. Nabedryk, E. (1996) in *Infrared Spectroscopy of Biomolecules* (Mantsch, H. H., and Chapman, D., Eds) pp 39−81, Wiley-Liss, New York.
12. Siebert, F. (1993) in *Biomolecular Spectroscopy* (Clark, R. J. H., and Hester, R. E., Eds.) Part A, pp 1−54, John Wiley & Sons, Chichester.
13. Maeda, A., Kandori, H., Yamazaki, Y., Nishimura, S., Hatanaka, M., Chon, Y.-S., Sasaki, J., Needleman, R., and Lanyi, J. K. (1997) *J. Biochem. 121*, 399−406.
14. Noguchi, T., Ono, T., and Inoue, Y. (1992) *Biochemistry 31*, 5953−5956.
15. Noguchi, T., Ono, T., and Inoue, Y. (1993) *Biochim. Biophys. Acta 1143*, 333−336.
16. Noguchi, T., Ono, T., and Inoue, Y. (1995) *Biochim. Biophys. Acta 1228*, 189−200.
17. Noguchi, T., Ono, T., and Inoue, Y. (1995) *Biochim. Biophys. Acta 1232*, 59−66.
18. Noguchi, T., Inoue, Y., and Tang, X.-S. (1997) *Biochemistry 36*, 14705−14711.
19. Noguchi, T., Inoue, Y., and Tang, X.-S. (1999) *Biochemistry 38*, 10187−10195.
20. Noguchi, T., Sugiura, M., and Inoue, Y. (1999) in *Fourier Transform Spectroscopy* (Itoh, K., and Tasumi, M., Eds.) pp 459−460, Waseda University Press, Tokyo, Japan.
21. Onoda, K., Mino, H., Inoue, Y., and Noguchi, T. (2000) *Photosynth. Res. 63*, 47−57.
22. Noguchi, T., and Sugiura, M. (2000) *Biochemistry 39*, 10943−10949.
23. Zhang, H., Fischer, G., and Wydrzynski, T. (1998) *Biochemistry 37*, 5511−5517.
24. Chu, H.-A., Gardner, M. T., O'Brien, J. P., and Babcock, G. T. (1999) *Biochemistry 38*, 4533−4541.
25. Chu, H.-A., Gardner, M. T., Hillier, W., and Babcock, G. T. (2000) *Photosynth. Res.* (in press).
26. Chu, H.-A., Hillier, W., Law, N. A., and Babcock, G. T. (2000) *Biochim. Biophys. Acta* (in press).
27. Chu, H.-A., Hillier, W., Law, N. A., Sackett, H., Haymond, S., and Babcock, G. T. (2000) *Biochim. Biophys. Acta 1459*, 528−532.
28. Styring, S., and Rutherford, A. W. (1988) *Biochim. Biophys. Acta 933*, 378−387.
29. Sugiura, M., and Inoue, Y. (1999) *Plant Cell Physiol. 40*, 1219−1231.
30. Hienerwadel, R., Thibodeau, D., Lenz, F., Nabedryk, E., Breton, J., Kreutz, W., and Mäntele, W. (1992) *Biochemistry 31*, 5799−5808.
31. Haumann, M., and Junge, W. (1996) in *Oxygenic Photosynthesis: The Light Reactions* (Ort, D. R., and Yocum, C. F., Eds.) pp 165−192, Kluwer, Dordrecht, The Netherlands.
32. Schlodder, E., and Witt, H. T. (1999) *J. Biol. Chem. 274*, 30387−30392.

BI0023807